33rd Annual International Conference of the IEEE EMBS
Boston, Massachusetts USA, August 30 - September 3, 2011

A Theoretical Study for the Inverse Design of an Ellipsoidal Phased-array Breast Coil

Yu Li[1], Feng Liu[1], Ewald Weber[1], Mingyan Li[1], Wenlong Xu[2], and Stuart Crozier[1], *Member, IEEE*

Abstract—**Magnetic resonance imaging (MRI) is widely used in human breast cancer detection, and the advancement of the radio-frequency (RF) phased-array technology promises to further improve the diagnostic image quality. In this paper, an inverse design method is presented for the theoretical design of an ellipsoidal RF phased array coil for human breast MRI. The target field technique was used to analytically express the relationship between the current density and the magnetic field within a predefined region; the streamline function technique was subsequently utilized to find the coil winding patterns. Based on a spherical coordinate system, the method is extended from the conventional cylindrical shape to the more tailored ellipsoidal geometry, a linearly polarization field used as an example. The theoretical analysis and the preliminary results presented demonstrate the flexibility of the proposed method.**

I. Introduction

MRI is a powerful tool for noninvasively image soft tissues in the human body. RF coils play a key role in the MRI scanning procedure, including generating the pulse excitations to the sample and picking up the molecular information via the signal induction in the coils with a high signal to noise ratio (SNR). Due to its capability to image soft tissues with high sensitivity, MRI has been regularly applied for the diagnosis of human breast cancer, which is one of the most common cancers in females.

A variety of RF breast coils have been presented. At first, whole body volume coils were used for breast MRI scanning. Relatively poor SNR was obtained and volume coils were found to be less efficient for imaging local regions. Later, close-fitting surface coils were proposed for breast imaging, to improve the SNR and the image quality. A specialized breast receive coil, consisting of two saddle coils connected in a serial configuration, has been designed by McOwen and Redpath[1]. A multi-coil array composed of four small diameter, individual RF surface coils were developed for high resolution breast imaging[2]. Recently, a number of other breast phased array coils have been developed, which employ small sized, simple loop-coils, positioned as close as possible to the breast lesion[3].

Along with the proposals of novel coils, great efforts have been made to develop numerical inverse techniques to improve coil design. The inverse design methods have been reviewed firstly by Turner[4], and recently by Hidalgo-Tobon[5] for gradient coils design. This method was later employed by Fujita et al. for the design of the RF coils. Fujita and colleagues successfully demonstrated that the inverse method could be used for designing a prototype four-loop lumped-element RF coil for use in a 1.5 T MRI system [6]. The Inverse Method had been experimentally and theoretically validated as an approach to RF coil designs. The inverse coil design method was further expanded and implemented by Lawrence and collaborators in the design of high-frequency RF coils [7]. A full-wave approach is required at higher frequencies and this was achieved by Lawrence et al. by using the time-harmonic Green's function for obtaining an expression for the magnetic field, rather than the Biot-Savart law. By using a time-harmonic inverse method, Lawrence et al. successfully designed and constructed a novel asymmetric RF coil for 4.5 T MRI systems [7] and an open head/neck RF coil to operate in a clinical 2 T system [8]. While et al. [9] extend the work of Lawrence et al. by considering a more general form of the current density and a new regularization penalty function. In addition, it has been combined with other methods like the boundary element method in designing RF phased array coils[10], and the deformation method in designing breast RF phased array coils[11].

As mentioned above, dedicated surface RF coils are sensitive to signals close to the receiver coil, while fairly insensitive to signals further away, which can reduce the aliasing motion artifacts from the rest of the body and, consequently, enhance the image quality and improve the SNR. Therefore, closer-fitting RF phased-array coils, like conical or ellipsoidal-phased array breast coils, can realize the full benefit of a surface coil. Such geometries are more complex than the commonly used cylindrical systems, and design methods for these unusual geometries have rarely been reported.

In this study, we extend the inverse design model of While et al [12] further to extend breast RF phased array coils from cylindrical geometries to tailored shapes. The aim of this paper is to provide a theoretical design for a RF phased-array breast coil with ellipsoidal geometry.

II. Methodology

A. Target Electromagnetic Field Expression

In the inverse phased-array coil design approach, the Target Field Method is used to specify the target B_1 field on a specified target surface, located inside the field of view of the coil and to find a continuous current density distribution on a given coil geometry, normally a cylinder. In terms of the relationship between the field and the source, the target

[1]School of Information Technology and Electrical Engineering, University of Queensland, QLD 4072, Australia (e-mail Yu Li: yuli@itee.uq.edu.au).
[2]Department of Biomedical Engineering, China Jiliang University, China

magnetic field can be described by the source current density, J_s, which is distributed on the conductor surface, as

$$B(r) = f[\vec{j}_s(r')] \tag{1}$$

An arbitrary view point of the source is at *r'* and an arbitrary viewpoint for the target field is located at *r*.

Conventionally, the design of RF phased-array coil using inverse methods has been limited to cylindrical geometries. In this work, the shape of the phased-array coil is extended into ellipsoidal structures. The geometrical sketch of an ellipsoid is shown in Fig.1, and the ellipsoid lies coaxially with the z-axis. The υ-component varies in a pre-set span from υ_1 to υ_2 for prolate spherical coordinate system.

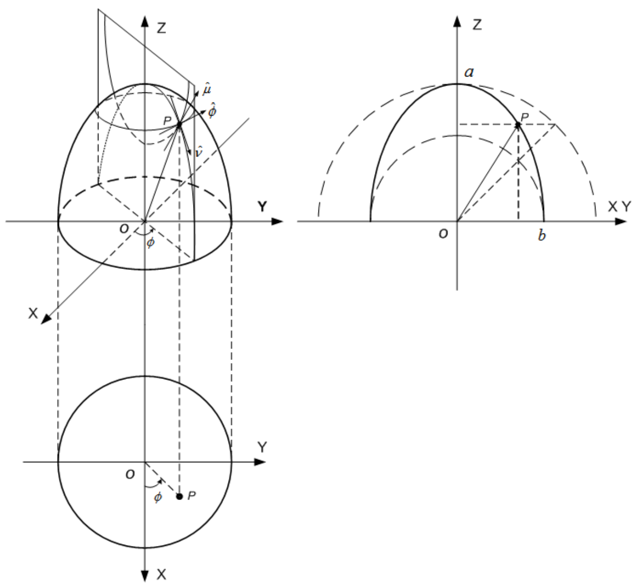

Fig. 1 Illustration of the ellipsoid surface and the relationship between Prolate Spheroidal coordinates with the Cartesian coordinate system

Point *P* is an arbitrary point on the surface of the ellipsoid surface shell with prolate spheroidal coordinates (μ, ν, ϕ), the corresponding Cartesian coordinates are ($\alpha \cdot \sinh\mu \cdot \sin\upsilon \cdot \cos\phi$, $\alpha \cdot \sinh\mu \cdot \sin\upsilon \cdot \sin\phi$, $\alpha \cdot \cosh\mu \cdot \cos\upsilon$). The semi-major axis is denoted by *a*; and the semi-minor axis is denoted by *b*. The Cartesian coordinates of the point *P* can be expressed as ($b \cdot \sin\upsilon \cdot \cos\phi$, $b \cdot \sin\upsilon \cdot \sin\phi$, $a \cdot \cos\upsilon$). The local orthogonal unit vectors, $\hat{\mu}$, $\hat{\nu}$ and $\hat{\phi}$, are in the directions of increasing μ, v and ϕ, respectively.

In terms of the prolate spheroidal coordinate, the spatial current densities $\bar{\jmath}(r')$ in components form can be expressed as

$$\begin{aligned}\vec{j}(r') &= \vec{j}_\mu(\mu',\nu',\phi')\hat{e}_{\mu'} + \vec{j}_\nu(\mu',\nu',\phi')\hat{e}_{\nu'} \\ &\quad + \vec{j}_\phi(\mu',\nu',\phi')\hat{e}_{\phi'}\end{aligned} \tag{2}$$

Because the α- and μ-component are constants for an ellipsoid phased-array design with a given dimension, the ellipsoid surface current density in a Cartesian coordinate can be expressed as

$$\begin{aligned}\vec{j}(r') &= \vec{j}_\nu(\mu',\nu',\phi')\hat{e}_{\nu'} + \vec{j}_\phi(\mu',\nu',\phi')\hat{e}_{\phi'} \\ &= \begin{bmatrix}\cos\phi' \cdot \cos(\tan^{-1}(\tan(\nu') \cdot \coth(\mu'))) \cdot \vec{j}_\nu(\mu',\nu',\phi') - \\ \sin\phi' \, \vec{j}_\phi(\mu',\nu',\phi')\end{bmatrix} \hat{e}_x \\ &\quad + \begin{bmatrix}\sin\phi' \cdot \cos(\tan^{-1}(\tan(\nu') \cdot \coth(\mu'))) \cdot \vec{j}_\nu(\mu',\nu',\phi') + \\ \cos\phi' \, \vec{j}_\phi(\mu',\nu',\phi')\end{bmatrix} \hat{e}_y \\ &\quad + \left[-\sin(\tan^{-1}(\tan(\nu') \cdot \coth(\mu'))) \cdot \vec{j}_\nu(\mu',\nu',\phi')\right] \hat{e}_z\end{aligned} \tag{3}$$

Here, the distance between the source and the field point can be expressed as

$$\begin{aligned}\ell &= |r' - r| \\ &= \sqrt{\begin{aligned}&(\alpha \cdot \sinh\mu' \cdot \sin\nu' \cdot \cos\phi' - x)^2 + (\alpha \cdot \sinh\mu' \cdot \sin\nu' \cdot \sin\phi' - y)^2 + \\ &(\alpha \cdot \cosh\mu' \cdot \cos\nu' - z)^2\end{aligned}}\end{aligned} \tag{4}$$

The mapping of the coordinate system between this work and the horizontal MRI system is, *x* to *Z*, *y* to *X* and *z* to *Y*. Where (*x, y, z*) are the three local coordinate components of this work, and (*X, Y, Z*) are the three coordinate components of the horizontal MRI system. Therefore, the y-component of the magnetic field (H_y) (in local coordinates) that is considered in the work is equivalent to the H_X in the system coordinates. The expressions for the *y*-component of the induced magnetic field vector at any field point (*x, y, z*) in Cartesian coordinates are expressed as

$$\begin{aligned}\vec{H}_y(x,y,z) &= \frac{1}{4\pi} \iint_\Sigma e^{-i\alpha\ell} \left(\frac{i\alpha}{\ell^2} + \frac{1}{\ell^3}\right) (r' - r) \times \vec{j}(r') \, ds \\ &= \frac{1}{4\pi} \iint_\Sigma \begin{bmatrix} \vec{j}_\nu \begin{pmatrix} AC \cdot \cos\nu' \cdot \cos\phi' \cdot \cos\left(\tan^{-1}\left(CU \cdot \tan(\nu')\right)\right) \\ + AS \cdot \sin\nu' \cdot \cos\phi' \cdot \sin\left(\tan^{-1}\left(CU \cdot \tan(\nu')\right)\right) \\ - z \cdot \cos\phi' \cdot \cos\left(\tan^{-1}\left(CU \cdot \tan(\nu')\right)\right) \\ - x \cdot \sin\left(\tan^{-1}\left(CU \cdot \tan(\nu')\right)\right) \end{pmatrix} \\ + \vec{j}_\phi\left(z \cdot \sin\phi' - AC \cdot \cos\nu' \cdot \sin\phi'\right) \end{bmatrix} \\ &\quad \cdot e^{-i\alpha\ell} \left(\frac{i\alpha}{\ell^2} + \frac{1}{\ell^3}\right) ds\end{aligned} \tag{5}$$

where, $\begin{cases} SU = \sinh(\mu'); \\ CU = \cosh(\mu'); \end{cases}$ *and* $\begin{cases} AS = \alpha \cdot \sinh(\mu'); \\ AC = \alpha \cdot \cosh(\mu'); \end{cases}$

B. Streamline functions

The corresponding components of the ellipsoid surface current density $\bar{J}_s$ are expressed in a transform of the Fourier series as

$$\vec{j}_{\nu,\phi} = \sum_m \sum_n S_{m,n}^{k,q} \cdot \sin\left[f(\mu,\nu',\phi',m,n)\right] \cos\left[g(\mu,\nu',\phi',m,n)\right] \tag{6}$$

Here, S_{mn}^{kq} (*m=1: M, n=1: N, k=1: K, q=1: Q*) is the Fourier coefficient and *m* and *n* are positive integers. The coil region was divided into *K*Q* sub-regions, with *K* divisions in ϕ and *Q* divisions in *v*. The current density must satisfy the continuity equation and be divergence-free $\nabla \cdot \bar{\jmath} = 0$. These two components of the divergence-free current density can be related via the stream function $\bar{S}(\nu', \phi')$, by means of the equations

$$\begin{cases} \vec{j}_{\nu}^{kq}(\nu',\phi') = \dfrac{-1}{\sin\nu'\cdot\sqrt{\sin^2\mathrm{h}\,\mu+\sin^2\nu'}}\cdot\dfrac{\partial\bar{S}}{\partial\phi'} \\ \vec{j}_{\phi}^{kq}(\nu',\phi') = \dfrac{\sinh\mu}{\left(\sin^2\mathrm{h}\,\mu+\sin^2\nu'\right)}\cdot\dfrac{\partial\bar{S}}{\partial\nu'} \end{cases} \tag{7}$$

with the corresponding streamline function being given by

$$\bar{S}(\nu',\phi') = \sum_{n=1}^{N}\sum_{m=1}^{M} S_{mn}^{kq}\sin\left(\frac{n\pi Q(\nu'-\nu_1)}{(\nu_2-\nu_1)}\right)\sin\left(\frac{mK\phi'}{2}\right) \tag{8}$$

Hence, these two components of the current density in the (k, q) region were chosen to be

$$\begin{cases} \vec{j}_{\nu}^{kq}(\nu',\phi') = \dfrac{-mK}{2\sin\nu'\cdot\sqrt{\sin^2\mathrm{h}\,\mu+\sin^2\nu'}}\bullet \\ \qquad \displaystyle\sum_{n=1}^{N}\sum_{m=1}^{M} S_{mn}^{kq}\sin\left(\frac{n\pi Q(\nu'-\nu_1)}{(\nu'-\nu_1)}\right)\cos\left(\frac{mK\phi'}{2}\right) \\ \vec{j}_{\phi}^{kq}(\nu',\phi') = \dfrac{n\pi Q\sinh\mu}{(\nu_2-\nu_1)(\sin^2\mathrm{h}\,\mu+\sin^2\nu')}\bullet \\ \qquad \displaystyle\sum_{n=1}^{N}\sum_{m=1}^{M} S_{mn}^{kq}\cos\left(\frac{n\pi Q(\nu'-\nu_1)}{(\nu'-\nu_1)}\right)\sin\left(\frac{mK\phi'}{2}\right) \end{cases} \tag{9}$$

where $\begin{cases} \nu' \in [\nu_1+(q-1)\dfrac{(\nu_2-\nu_1)}{Q}, \nu_1+q\dfrac{(\nu_2-\nu_1)}{Q}] \\ \phi' \in [(k-1)\dfrac{2\pi}{K}, k\dfrac{2\pi}{K}] \end{cases}$, and $\begin{cases} k=1:K \\ q=1:Q \end{cases}$.

C. *System matrix equation*

The series expressions for $\bar{J}_{\nu}^{kq}(\nu',\phi')$ and $\bar{J}_{\phi}^{kq}(\nu',\phi')$ given by the equations 9 are substituted into Equation 5; the y-components of the magnetic field induced at any (x, y, z) field point by the phased-array coil as a system equation

$$\vec{H}_y(x,y,z) = \sum_{n=1}^{N}\sum_{m=1}^{M}\sum_{q=1}^{Q}\sum_{k=1}^{K} I_{mn}^{kq}(\nu',\varphi',x,y,z)\,S_{mn}^{kq} \tag{10}$$

where, $I_{mn}^{kq} = (\nu',\phi',x,y,z)$ is the intermediate integral function, which is expressed as

$$\begin{aligned} I_{mn}^{kq}(x,y,z) &= \frac{1}{4\pi}\iint_{\Sigma} e^{-i\alpha\ell}\left(\frac{i\alpha}{\ell^2}+\frac{1}{\ell^3}\right)(r'-r)\times\vec{j}(r')\,ds \\ &= \frac{1}{4\pi}\iint_{\Sigma}\left[\begin{array}{l} \vec{j}_{\nu}\left(\begin{array}{l} AC\cdot\cos\nu'\cdot\cos\phi'\cdot\cos\left(\tan^{-1}\left(CU\cdot\tan(\nu')\right)\right) \\ +AS\cdot\sin\nu'\cdot\cos\phi'\cdot\sin\left(\tan^{-1}\left(CU\cdot\tan(\nu')\right)\right) \\ -z\cdot\cos\phi'\cdot\cos\left(\tan^{-1}\left(CU\cdot\tan(\nu')\right)\right) \\ -x\cdot\sin\left(\tan^{-1}\left(CU\cdot\tan(\nu')\right)\right) \end{array}\right) \\ +\vec{j}_{\phi}\left(z\cdot\sin\phi'-AC\cdot\cos\nu'\cdot\sin\phi'\right) \end{array}\right]\cdot e^{-i\alpha\ell}\left(\frac{i\alpha}{\ell^2}+\frac{1}{\ell^3}\right)ds \\ &= \frac{1}{4\pi}\int_{(k-1)\frac{2\pi}{K}}^{k\frac{2\pi}{K}}\int_{\nu_1+(q-1)\frac{(\nu_2-\nu_1)}{Q}}^{\nu_1+q\frac{(\nu_2-\nu_1)}{Q}} \left[\begin{array}{l} \vec{j}_{\nu}\left(\begin{array}{l} AC\cdot\cos\nu'\cdot\cos\phi'\cdot\cos\left(\tan^{-1}\left(CU\cdot\tan(\nu')\right)\right) \\ +AS\cdot\sin\nu'\cdot\cos\phi'\cdot\sin\left(\tan^{-1}\left(CU\cdot\tan(\nu')\right)\right) \\ -z\cdot\cos\phi'\cdot\cos\left(\tan^{-1}\left(CU\cdot\tan(\nu')\right)\right) \\ -x\cdot\sin\left(\tan^{-1}\left(CU\cdot\tan(\nu')\right)\right) \end{array}\right) \\ +\vec{j}_{\phi}\left(z\cdot\sin\phi'-AC\cdot\cos\nu'\cdot\sin\phi'\right) \end{array}\right]\cdot e^{-i\alpha\ell}\left(\frac{i\alpha}{\ell^2}+\frac{1}{\ell^3}\right) \\ &\quad \cdot\sin\nu'\cdot(a\cdot\sinh\mu)\cdot\sqrt{\left((a\cdot\sinh\mu)\cdot\cos\nu'\right)^2+\left((a\cdot\cosh\mu)\cdot\sin\nu'\right)^2}\,d\nu'd\phi' \\ &= \frac{AS}{4\pi}\int_{(k-1)\frac{2\pi}{K}}^{k\frac{2\pi}{K}}\int_{\nu_1+(q-1)\frac{(\nu_2-\nu_1)}{Q}}^{\nu_1+q\frac{(\nu_2-\nu_1)}{Q}} \left[\begin{array}{l} \dfrac{-mK}{2\sin\nu'\cdot\sqrt{\sin^2\mathrm{h}\,\mu+\sin^2\nu'}} \\ \left(\begin{array}{l} AC\cdot\cos\nu'\cdot\cos\phi'\cdot\cos\left(\tan^{-1}\left(CU\cdot\tan(\nu')\right)\right) \\ +AS\cdot\sin\nu'\cdot\cos\phi'\cdot\sin\left(\tan^{-1}\left(CU\cdot\tan(\nu')\right)\right) \\ -z\cdot\cos\phi'\cdot\cos\left(\tan^{-1}\left(CU\cdot\tan(\nu')\right)\right) \\ -x\cdot\sin\left(\tan^{-1}\left(CU\cdot\tan(\nu')\right)\right) \end{array}\right) \\ \cdot\sin\left(\dfrac{n\pi Q(\nu'-\nu_1)}{(\nu_2-\nu_1)}\right)\cos\left(\dfrac{mK\phi'}{2}\right) \\ + \\ \dfrac{n\pi Q\sinh\mu}{(\nu_2-\nu_1)(\sin^2\mathrm{h}\,\mu+\sin^2\nu')}\cdot\left(z\cdot\sin\phi'-AC\cdot\cos\nu'\cdot\sin\phi'\right) \\ \cdot\cos\left(\dfrac{n\pi Q(\nu'-\nu_1)}{(\nu_2-\nu_1)}\right)\sin\left(\dfrac{mK\phi'}{2}\right) \end{array}\right] \\ &\quad \cdot\sin\nu'\cdot\sqrt{(AS\cdot\cos\nu')^2+(AC\cdot\sin\nu')^2}\cdot e^{-i\alpha\ell}\left(\frac{i\alpha}{\ell^2}+\frac{1}{\ell^3}\right)d\nu'd\phi' \end{aligned} \tag{11}$$

The system equation 10 can be expressed in a matrix equation form, as

$$A \bullet X = H \tag{12}$$

When we set the sampling points on the target field as n, the dimension of the target field matrix H, the sensitivity matrix A and the Fourier coefficient matrix X is n-by-one, n-by-($K*Q*M*N$) and ($K*Q*M*N$)-by-one, respectively. The value of the elements in the sensitivity matrix A is determined by the integral equation 11.

D. *Solving the system equation and constructing coil contours*

In the system equation, matrix A presents an ill-posed condition. Because this is typically an inverse problem, a regularization method was implemented to find a practical and reasonable solution for the system matrix equation[13]. Once the system matrix function was solved properly and the current density is calculated from this pre-set RF field, stream function techniques are employed to make discrete the continuous current distributions. The streamline function can be contoured and these patterns are used to design an RF coil that has approximately the same current density distributions as the original theoretical current distribution calculated from the inverse technique. Hence, the appropriate coil-winding pattern can be achieved. Depicted in Figure 2 is a preliminary result of a two-element ellipsoidal breast coil. The focus of ellipse is 120mm and the semiminor axis is 80mm.

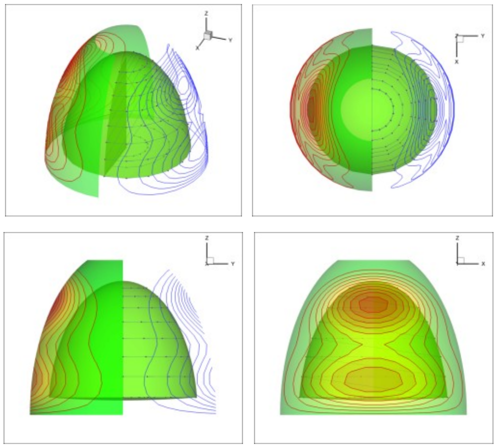

Fig. 2 The coil-winding pattern of a two-element ellipsoid breast phased-array obtained from a streamline contour

The green half-ellipsoid inside the array coil is the target field region which is 80% of the size of the coil. The red points on the surface of the target region are the sampling points. Red wires indicate reversed current flow with respect to blue.

III. Conclusion

In this work, a theoretical inverse method for the design ellipsoidal phased-array breast coils was proposed. The electromagnetic field problem in MRI was modeled using analytical methods. Compared to the conventional cylindrical coil design, these coils tend to conform more closely to some parts of the body. Additionally, the inverse coil design method introduced in this work can not only be used in phased-array coil design work, but can also be extended for the analysis and design of local gradient coils, such as head or breast gradient coils. Future work will be to improve the performance of the coil structures with the consideration of coil-coil coupling issues and particularly load-coil interactions in high field. A prototype will also be built to test the practical feasibility of the design method.

Appendix

As shown in Fig. 3, the prolate spheroidal coordinate system is a three-dimensional orthogonal coordinate system, which is resulted from rotating a spheroid around its major axis, i.e., the axis on which the foci are located. Rotation around the other axis will produce the oblate spheroidal coordinates.

The most common definition of prolate spheroidal coordinates (μ, ν, ϕ) is:

$$\begin{cases} x=\alpha\cdot\sinh\mu\cdot\sin\nu\cdot\cos\phi \\ y=\alpha\cdot\sinh\mu\cdot\sin\nu\cdot\sin\phi \\ z=\alpha\cdot\cosh\mu\cdot\cos\nu \end{cases} \quad \text{(a1)}$$

Where μ is a nonnegative real number and ν varies from 0 to 2π. The azimuthal angle ϕ belongs to the interval $[0,2\pi)$, and α is the half foci. There exists the trigonometric identity

$$\frac{z^2}{\alpha^2\cosh^2\mu}+\frac{x^2+y^2}{\alpha^2\sinh^2\mu}=\cos^2\nu+\sin^2\nu=1 \quad \text{(a2)}$$

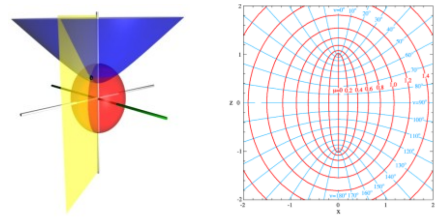

Fig. 3 The prolate spheroidal coordinate system (en.wikipedia.org)

which shows that the surfaces of constant μ form the prolate spheroids, since they are ellipses rotated about the axis joining their foci. Similarly, the hyperbolic trigonometric identity is existed too as:

$$\frac{z^2}{\alpha^2\cos^2\nu}-\frac{x^2+y^2}{\alpha^2\sin^2\nu}=\cosh^2\mu-\sinh^2\mu=1 \quad \text{(a3)}$$

which shows that surfaces of constant ν form the hyperboloids of revolution. Therefore, 'α' and 'μ' are two constants for an ellipsoidal shell with given dimensions, while variable ν and ϕ are two coordinate components.

Acknowledgements

This work was supported by the Australia research council and Science and Technology Department of Zhejiang province, China, project ID- 2010C14010.

References

[1] McOwan, P.W. and T.W. Redpath, *A specialised receiver coil for NMR imaging of female breasts.* Phys. Med. Biol., 1987. 32(2): p. 259-63.

[2] Insko, E.K., T.J. Connick, M.D. Schnall, and S.G. Orel, *Multicoil array for high resolution imaging of the breast.* Magn. Reson. Med., 1997. 37(5): p. 778-84.

[3] *Magnetic resonance imaging array coil system and method for breast imaging.* U.S. Pat. US7084631, 2006.

[4] Turner, R., *Gradient coil design: a review of methods.* Magn. Reson. Imaging, 1993. 11(7): p. 903-20.

[5] Hidalgo-Tobon, S.S., *Theory of gradient coil design methods for magnetic resonance imaging.* Concept. Magn. Reson. A, 2010. 36A(4): p. 223-242.

[6] Brown, R.W., H. Fujita, S.M. Shvartsman, M.R. Thompson, M.A. Morich, L.S. Petropoulos, and V.C. Srivastava, *New applications of inverse methods in the design of MRI coils.* International Journal of Applied Electromagnetics and Mechanics, 1998. 9(3): p. 277-290.

[7] Lawrence, B.G., S. Crozier, D.D. Yau, and D.M. Doddrell, *A time-harmonic inverse methodology for the design of RF coils in MRI.* IEEE Trans Biomed Eng, 2002. 49(1): p. 64-71.

[8] Lawrence, B.G., S. Crozier, G. Cowin, and D.D. Yau, *An inverse design of an open, head/neck RF coil for MRI.* IEEE Trans Biomed Eng, 2002. 49(9): p. 1024-30.

[9] While, P.T., L.K. Forbes, and S. Crozier, *A time-harmonic target-field method for designing unshielded RF coils in MRI.* Measurement Science & Technology, 2005. 16(4): p. 997-1006.

[10] Shou, G.F., L. Xia, F. Liu, M.H. Zhu, Y. Li, and S. Crozier, *MRI coil design using boundary-element method with regularization technique: a numerical calculation study.* IEEE Trans. Magn., 2010. 46(4): p. 1052-1059.

[11] Li, Y., F. Liu, E. Weber, B. Li, and S. Crozier, *Inverse Design of a Phased-Array Coil for Breast Magnetic Resonance Imaging.* Concept. Magn. Reson. B, 2009. 35B(4): p. 221-231.

[12] While, P.T., L.K. Forbes, and S. Crozier, *An inverse method for designing RF phased array coils in MRI-theoretical considerations.* Meas. Sci. Technol., 2007. 18: p. 245-259.

[13] Li, Y., H. Wang, F. Liu, B.K. Li, G. Shou, E. Weber, and S. Crozier, *A comparison study of regularization techniques on the theoretical design of phased array RF coils in MRI.* Conf Proc IEEE Eng Med Biol Soc, 2008. 2008: p. 439-42.